ARTICLE

Development of Quercetin-modified silver nanoparticles for paper-based detection of methomyl pesticide

Isabella Marie S. Vasquez[1], Victor I. Escalona[1], Mark Alexis O. Liscano[1], and Angelica A. Tabamo*[1,2]

[1]Department of Chemistry, College of Science, Tarlac State University, Tarlac City 2300, Philippines
[2]Center for Natural Products Research, Tarlac State University, Tarlac City 2300, Philippines

ABSTRACT

Carbamates are among the widely used agrochemicals due to their broad spectrum of activity, high pesticide efficiency, and relatively lower environmental half-life. Although they offer several agricultural benefits, post-harvest carbamate residues in fruits and vegetables pose significant health risks. Traditional methods such as chromatography and enzyme inhibition assays are well-established for the detection of pesticides. However, these methods tend to be resource-intensive, often requiring sophisticated equipment and advanced technical expertise, which can limit their applicability in routine agricultural settings when quick testing is essential. In this study, a paper-based colorimetric device was developed by impregnating quercetin-modified Silver nanoparticles (Q-AgNPs) onto a paper substrate for the detection of the carbamate pesticide, methomyl. The optimum pH of the test solutions was found to be 7.43-8.00, while the optimum dipping time is 60 s and the optimum drying time is up to 120 min. Digital images of the developed strips were captured using a high-resolution scanner and analyzed through ImageJ software, providing a semi-quantitative measurement of methomyl concentration in the samples. The detection limit was found to be 2.621 mg/L, with a limit of quantification (LOQ) of 7.943 mg/L. Additionally, the percent recovery of the spiked samples was estimated to be 93 to 95%, further verifying the efficiency of the sensor in detecting methomyl residues. Furthermore, the concentrations detected by the paper-based device were verified by UV-Vis spectrophotometry, supporting its potential as a screening tool for semi-quantitative on-site pesticide residue analysis, promoting safer agricultural practices and consumer health protection.

*Corresponding author
Email Address: **aatabamo@tsu.edu.ph**
Date received: 04 February 2026
Date revised: 03 April 2026
Date accepted: 25 May 2026
DOI: https://doi.org/10.54645/2026191JHT-36

INTRODUCTION

Pesticides are chemical substances used in agriculture to protect crops against a wide range of pest and improve yield. These pesticides are generally classified as neonicotinoids, organochlorines, pyrethroids, organophosphates, and carbamates, which have varying persistence in the environment (United States Environmental Protection Agency [EPA], 2006). Over the past three decades, carbamate pesticides have gained popularity in crop protection, especially during later stages of crop growth, due to their broad spectrum of effectiveness (Rowayshed, et al., 2013). The discovery of the first known carbamate compound dates to the mid-nineteenth century. Subsequently, in the 1960s and 1970s, numerous carbamates were synthesized for pesticidal purposes. Commonly used carbamate pesticides are N-methyl derivatives of carbamic acid, such as bendiocarb, carbaryl, carbofuran, methomyl, and several others (Gupta, 2014).

Although carbamates are generally less toxic than other pesticides, studies have indicated that they possess comparable levels of toxicity and are still regarded as hazardous, similar to organophosphates (Jali et al., 2024; Xia et al., 2024). N-methylcarbamate insecticides mostly cause acute toxicity by preventing the activity of acetylcholinesterase (AChE), which results in a buildup of acetylcholine (ACh) at cholinergic junctions. Many symptoms can result from overstimulating the body, such as muscarinic effects like increased salivation and gastrointestinal distress and nicotinic effects like muscle weakness and blurred eyesight. Serious poisoning can also result in coma and seizures, and central nervous system symptoms that may lead to death due to cardiorespiratory failure. Apoptosis, oxidative stress, and carcinogenesis are among the various bodily systems that these pesticides may impact (Moon, et al., 2012). For this reason, some pesticides like carbamates are either regulated or banned in various parts of Europe and the United States (US) (European Parliament and Council of the European Union, 2009). However, these chemicals are still being used in the Philippines, particularly in regions with extensive crop and vegetable cultivation such as the

KEYWORDS

Paper-based device, Silver Nanoparticles, Quercetin, Carbamate, Methomyl, Pesticide

Mt. Province, Ifugao in the Cordilleras, and Benguet province (Ngidlo, 2013; Fertilizer and Pesticide Authority [FPA], 2024).

A few of the established methods for pesticide analysis include chromatography coupled with mass spectrometry and enzyme inhibition techniques like ELISA are renowned for their accuracy and sensitivity (Hermanto et al., 2023). However, such traditional methods are limited because they require costly instruments, and the preparation of samples involves complex procedures and needs specially trained operators. The interest in simplifying the detection of substances such as pesticides is emphasized by the development of chemical and biosensors, as well as the increase in attention to the paper-based ones (Javed, et al., 2020). These detectors are especially beneficial in resource-limited settings due to their affordability, simple production, and minimal need for specialized equipment. They enable rapid response in remote or outdoor applications since they allow real-time and in-field detection with observable color changes (Hermanto, et al., 2023; Javed, et al., 2020).

Other recent studies have also worked on the optimization of the performance of such paper-based detectors by embedding metal nanoparticles, which are identified to possess both optical and electrochemical characteristics. The unique localized surface plasmon resonance (LSPR), thermal or electrochemical properties of silver nanoparticles (AgNPs) are widely used in nanosensors, especially when detecting pesticide residues in different samples. They may also be produced by top-down synthesis done by breaking down bulk material via physical force; or by bottom-up synthesis done by the chemical reduction of silver salts, but the most widespread method is the latter (Hermanto, et al. 2023). Using capping and stabilizing agents can help in the reduction of silver salts to produce silver nanoparticles and increase their functionality for different applications. One of these capping agents is quercetin, a flavonoid which was proven to effectively reduce silver ions (Chen, et al., 2020, Pandian et al., 2021).

In this paper, we developed a paper-based colorimetric sensor to detect a carbamate pesticide, methomyl, in real samples by impregnating paper strips with the prepared quercetin-capped silver nanoparticles.

MATERIALS AND METHODS

Apparatus

The synthesized silver nanoparticles (AgNPs) were confirmed using a UV–VisF spectrophotometer (Shimadzu UV-1800) and the changes in the functional groups were determined using Fourier Transform Infrared (ATR-FT-IR) spectroscopy (Shimadzu IRAffinity-1S), within a wavenumber range of 4000-700 cm^{-1} with a resolution of 4 cm^{-1}, and 20 scans (Bordbar et al. 2020; Tasca & Antiochia, 2020). Test strip images were captured with a CanoScan LiDE300 flatbed scanner and analyzed using ImageJ software (version 1.51n, National Institutes of Health, USA).

Fabrication of the Paper-based sensor

Synthesis of Quercetin-modified Silver Nanoparticles (Q-AgNPs)
A 2.5 mL aliquot of 1.0 mM quercetin was added dropwise to 250.0 mL of 1.0 mM $AgNO_3$ solution, with constant stirring at 65 °C for one hour at pH 8. During this process, silver ions (Ag^+) were reduced to elemental silver (Ag^0), causing the solution to turn yellowish-brown. The resulting Q-AgNPs solution was filtered using a 0.22 µm syringe filter, after which, 30.0 mL of 0.1 M Tris buffer was added for every 50.0 mL of Q-AgNPs solution (Bordbar et al., 2020).

Fabrication of the Test Strips
The paper-based device was prepared using Whatman Grade No. 1 filter paper, cut into 1 cm × 4 cm strips. These paper strips were impregnated with the synthesized Q-AgNPs in 0.1 M Tris buffer solution for five minutes, then air-dried for two hours using a hanger with clips and stored in transparent plastic ziplock bags until further testing.

Colorimetric Analysis

The changes in the color were analyzed and calculated using ImageJ software. The software translates the color intensity of the paper-based device to three numerical mean values referred to as red, green, and blue color elements. In this analysis, control strips with uniform color were first scanned to determine how well the scanner could generate consistent quantitative values for different hues of colors. This preparatory procedure ensures that the quantitative values are based on the changes in color or hues of the paper strips as determined by ImageJ and are not based on any scanning inconsistencies. The difference between pre-exposure and post-exposure values was calculated as:

$$\Delta R = \bar{R}_{after} - \bar{R}_{before}$$
$$\Delta G = \bar{G}_{after} - \bar{G}_{before}$$
$$\Delta B = \bar{B}_{after} - \bar{B}_{before}$$

In these equations, the differences in the red, green, and blue components are represented as ΔR, ΔG, and ΔB, respectively (Bordbar et al., 2020). The colorimetric response ΔRGB of the replicates was also generated using ImageJ and the average ΔRGB was calculated for each sample for better estimation of the observed color changes.

Optimization of the Paper-based device and Analyte Condition

The ability of the method to produce strips with repeatable color intensities is crucial for this study, hence, five (5) strips were fabricated and analyzed with ImageJ software to determine the reproducibility of the color intensities of the fabricated strips. The optimum pH of the test solutions was determined by immersing the strips in 25.0 mg/L methomyl solutions at various pH levels ranging from 3.0 to 11.0, adjusted with either 0.1 M NaOH or 0.1 M HCl. The dipping time (5 s, 15 s, 30 s, and 60 s) and drying time was monitored to determine the optimal conditions for color intensity stabilization. The stability of the test strips after 2, 24, and 48 hours of storage, after exposure to methomyl, and the reproducibility of the color intensities of the strips at varying methomyl concentrations (0.1, 1.0, 5.0, and 15.0 mg/L) were also analyzed to ensure consistent sensor response. In the comparison of results, one-way Analysis of Variance (ANOVA) was used to determine the significant differences of the mean ΔRGB response values among the different levels of pH, dipping time, and drying time.

Method Validation

Determination of Linear Range, Limit of Detection (LOD), and Limit of Quantification (LOQ)
Ten (10) standard methomyl solutions with concentrations ranging from 0.075 to 15.00 mg/L were prepared to establish the linear range. Each concentration was tested in five (5) trials, and the mean color intensities of the test strips were determined.

The limit of detection (LOD) was calculated using the formula LOD =3.3 × s/m, where s is the residual standard deviation of the regression and m is the slope of the calibration curve based on the assumed range of the LOD value. Similarly, the limit of quantification (LOQ) was calculated as LOQ = 10s/m.

Ultraviolet-Visible Spectrophotometry Analysis

A comparative analysis was conducted using UV-Vis spectroscopy to verify the response of the paper-based device. Distilled water was used as a solvent blank for the baseline correction of the analysis. The maximum wavelength of absorption of the methomyl and Q-AgNPs was measured, and standard solutions with various concentrations were prepared with concentrations ranging from 0.075 to 15.0 mg/L to generate the calibration curve. Afterwards, 0.4 mL of Q-AgNPs was added for every 10 mL of the solution. Subsequently, the linearity, limits of detection (LOD), and limit of quantification (LOQ) were also determined in this analysis.

Spiked-Real Sample Analysis

Preparation and Analysis of the Methomyl-Spiked Samples
In this study, eggplant was selected as the matrix to show the ability of the paper-based device to detect methomyl. The eggplants were harvested from homegrown plants, free from pesticides, prior to spiking. Initially, the eggplants were thoroughly rinsed with distilled water and were dried by patting the surface with tissue and air-drying.

Once dried, 50.0 grams of eggplant were blended with 50.0 mL of distilled water. Subsequently, 125 mL of a 100 mg/L methomyl solution was added to the blended mixture, which was then diluted to a final volume of 500 mL, yielding 25 mg/L methomyl-spiked sample. The solution was stirred continuously for 30 minutes and sonicated for 5 minutes to ensure proper mixing. After sonication, the sample was divided into two portions and further diluted to prepare methomyl-spiked samples with concentrations of 5 mg/L and 10 mg/L. Each sample underwent two rounds of sonication, mixing, and vacuum filtration to ensure uniform distribution of the pesticide and the removal of any residual particulate matter, resulting in a clear and homogeneous solution. The fabricated paper-based device was used to detect methomyl in the real samples, with the optimized conditions for pH, dipping time and drying time applied for each. The mixtures were then subjected to UV-Vis Spectroscopy to determine the concentration of methomyl.

Analysis of the Methomyl-Spiked Samples using UV-Vis Spectrophotometry
The multiple standard addition method was employed to minimize matrix effects in the eggplant samples during the determination of methomyl concentration. In this approach, 5 mL aliquots of eggplant extract were transferred to 50-ml volumetric flasks, and varying volumes of a 50 mg/L methomyl stock solution were added to achieve final concentrations ranging from 0.075 to 12 mg/L. These solutions were then analyzed using a UV-Vis spectrophotometer, measuring absorbance at the wavelength corresponding to the maximum absorption of the solution produced from the reaction of methomyl and Q-AgNPs. A calibration curve was constructed, and the concentration of methomyl was determined from the x-intercept of the linear regression equation derived from the calibration curve, with necessary corrections for dilution factors.

RESULTS AND DISCUSSION

Synthesis of Quercetin-Modified Silver Nanoparticles

The synthesis of Quercetin-modified silver nanoparticles (Q-AgNPs) was carried out through a bottom-up method. Initially, the silver nitrate was dissolved in water, producing a solution rich in silver ions (Ag^+). Quercetin was then added, where it interacted directly with these ions. Its phenolic hydroxyl groups acted as natural reducing agents (Chahardoli et al., 2021) to convert the silver ions into elemental silver (Ag^0) (Figure 1A). Quercetin's aromatic rings then stabilized the electron transfer, allowing small silver clusters, or nuclei, to gradually grow into nanoparticles (Figure 1B) (Rohit & Kailasa, 2014; Mohammadi & Khayatian, 2017; Bhutto et al., 2018).

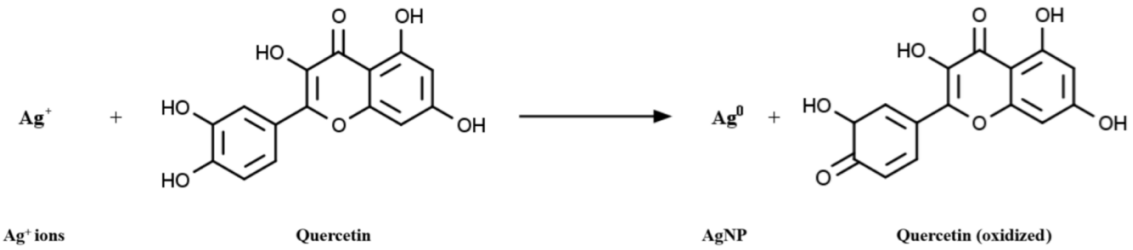

1A. Reduction of Ag+ ions to AgNPs

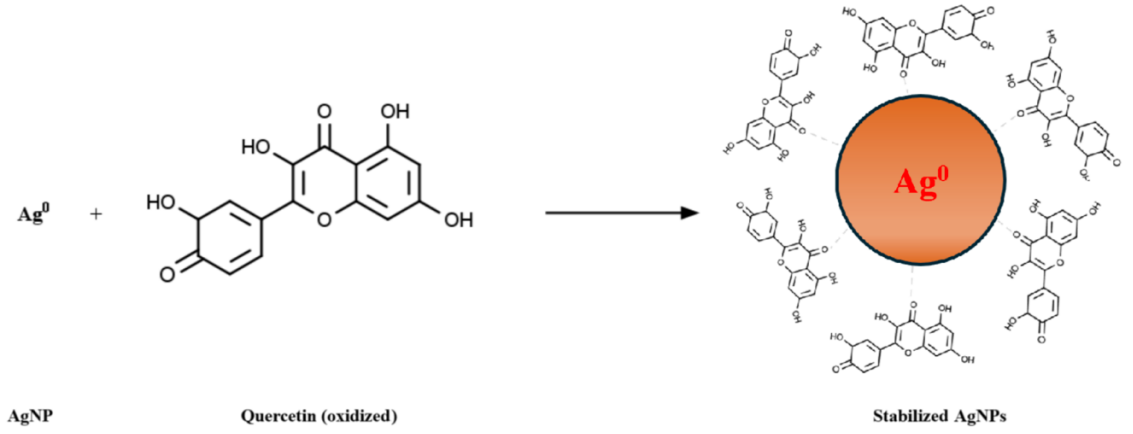

1B. Stabilization of AgNPs

Figure 1: Synthesis of Q-AgNPs.

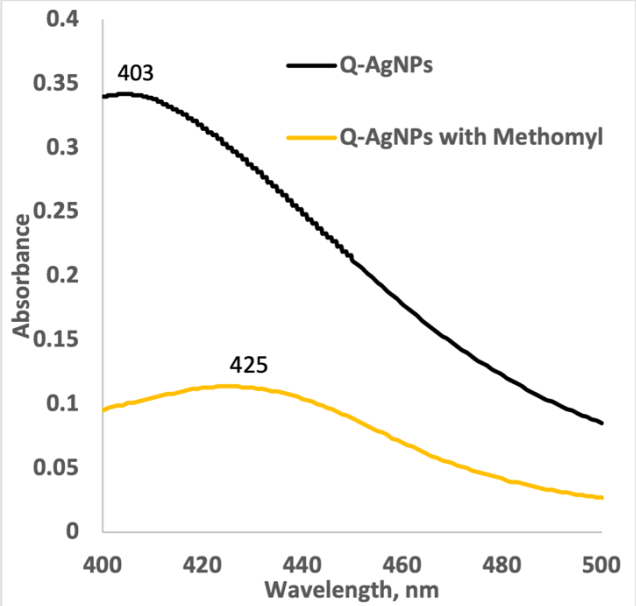

Figure 2: Absorption spectrum of the synthesized Q-AgNPs and Q-AgNPs after interaction with Methomyl.

The synthesized Q-AgNPs were confirmed using the UV-Vis Spectrophotometer. The absorption spectrum (Figure 2) of the synthesized Q-AgNPs showed a maximum absorption at 403 nm, which shifted to 425 nm after interaction with methomyl. This shift is indicative of changes in the local refractive index and electron density around the nanoparticles, which suggests that methomyl interacted with the surface of the Q-AgNPs, altering their optical properties (Tasca and Antiochia, 2020; Jana et al., 2016).

The $AgNO_3$ solution (Figure 3A) showed prominent peaks at approximately 3325 cm^{-1} due to O-H stretching, at 1635 cm^{-1} due to O-H bending, and 1342 cm^{-1} due to the stretching of the Nitrate ion (Mahitha et al., 2011; Khandel et al., 2018; Upadhyay et al., 2019; Mistry et al., 2021; Zhang et al., 2021). On the other hand, the IR spectrum of quercetin (Figure 3B) exhibited prominent peaks at signals around 3325.28 cm^{-1}, indicative of phenolic or hydroxyl groups (O-H stretching vibrations), a C=O stretching from carbonyl group, likely from a conjugated ketone at 1651 cm^{-1}; a C–O stretching of the aromatic group and O-H bending between ~1420 cm^{-1} and ~1270 cm^{-1}, C–O stretching from ether or flavonoid structure at 1087.85 cm^{-1}; C-O-C at 1053.13 cm^{-1}, and an aromatic C–H bending (out-of-plane) at ~880 cm^{-1} (Rajhard, et al., 2021).

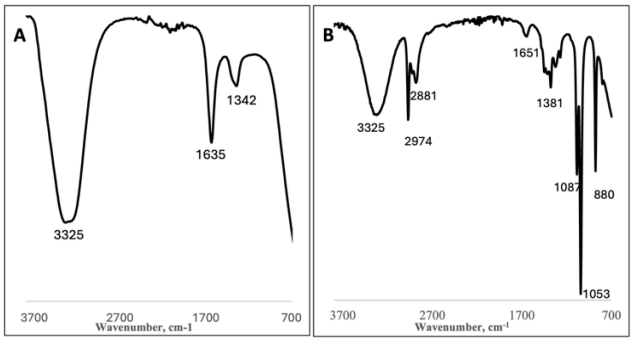

Figure 3: FT-IR Spectrum of (A) AgNO3 solution and (B) Quercetin in ethanol.

A comparison of the IR spectrum of $AgNO_3$ and Q-AgNPs (Figure 4) shows similarities at around ~3325 cm^{-1} and at ~1638.74 cm^{-1} (Mahitha et al., 2011; Khandel et. al, 2018; Mistry, et al., 2021), but the absence of a peak at around 1342 cm^{-1} is consistent with the removal of the nitrate-containing precursor following the formation of Ag nanoparticles. Quercetin not only reduced Ag^{+} but also acted as a capping agent, adsorbing onto the nanoparticle surfaces and providing stability by preventing aggregation, which helped transform small silver nuclei into nanoparticles (Upadhyay et al., 2019). A visible color change—from clear to dark brown—signaled the successful formation of colloidal silver nanoparticles (Bordbar et al., 2020). As shown in Figure 4, quercetin peaks are absent in the synthesized Q-AgNPs which is likely due to its relatively low concentration and the overlap with the AgNP background.

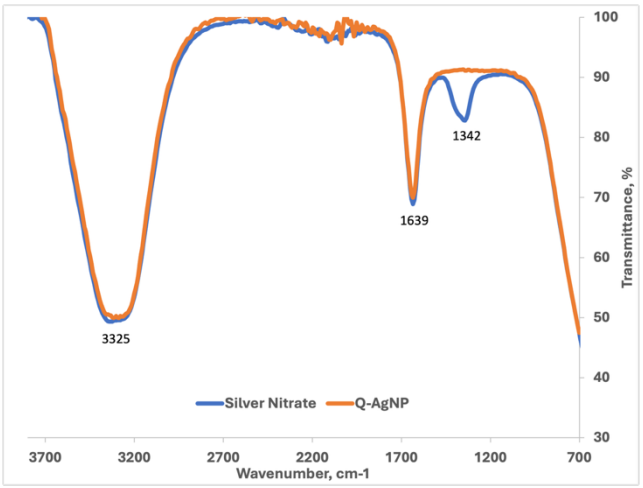

Figure 4: Superimposed FT-IR spectra of AgNO3 solution and Q-AgNPs.

Interaction Mechanism of Methomyl Detection

Methomyl primarily interacts with Q-AgNPs through non-covalent forces rather than forming direct chemical bonds. However, its functional groups—such as the carbonyl (C=O) and carbamate (-NHCOO) groups—can interact with the surface of Q-AgNPs . These interactions are likely facilitated by hydrogen bonding, coordination, or adsorption onto the nanoparticle surface. Specifically, the carbonyl oxygen and carbamate group of methomyl may coordinate to surface silver atoms, while the hydroxyl groups of quercetin may interact with methomyl's amide (-NH) or ester (-COO-) groups (Figure 5) (Bordbar et al., 2020; Dhavle et al., 2021; Hoang et al., 2021).

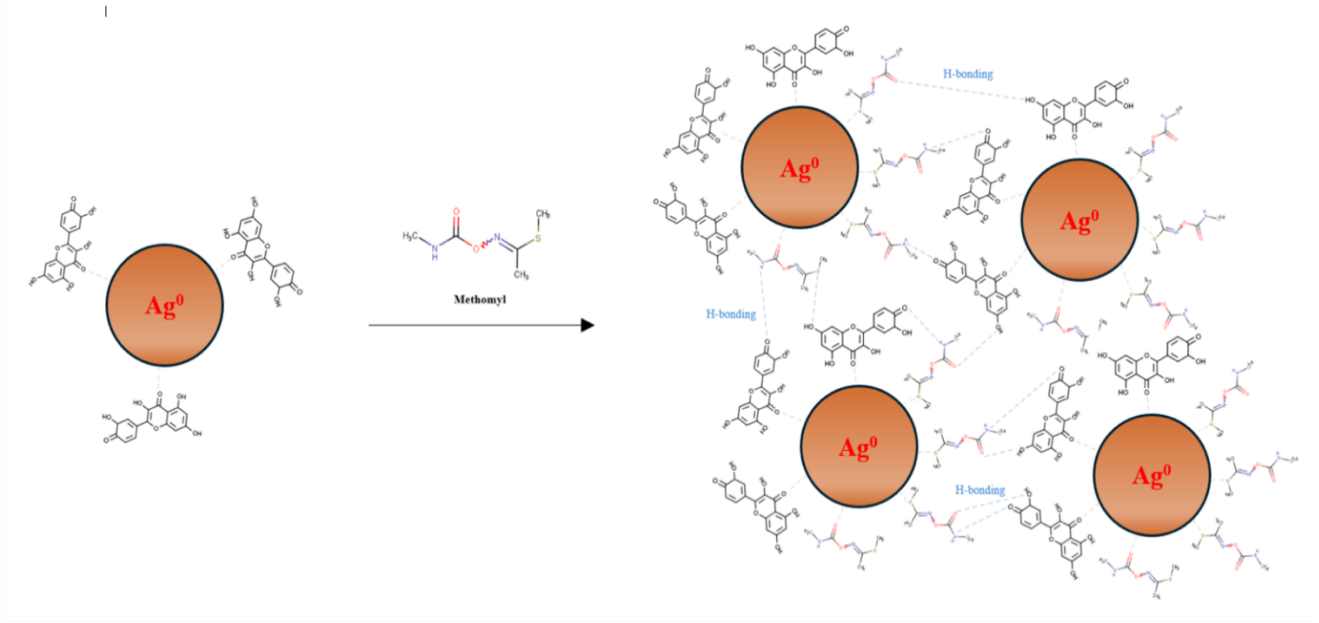

Figure 5: Proposed interaction mechanism of methomyl with Q-AgNPs.

The binding between methomyl and the quercetin layer can lead to a redistribution of charge, which affects the surface plasmon resonance (SPR) of the AgNPs. The shift in the maximum absorption peak from 403 nm to 425 nm at Figure 2 confirmed this effect. As a result of this interaction, a visible color change is observed on the paper-based detector, providing a straightforward visual confirmation of the presence of methomyl.

Optimization of the Paper-based device and Analyte Condition

Repeatability Test

Five (5) Q-AgNP strips, as shown in Figure 6A, were analyzed with ImageJ software to test the variation of the color intensities of the freshly prepared test strips. The ANOVA test revealed that the variations of the mean color intensities were not statistically significant with Fcalc = 1.7988 < Fcrit = 2.6207, which means that the method produces reproducible sensors.

pH

The findings on the effect of pH (Figure 6B) indicated that methomyl solutions with pH 7.43 and pH 8.00 showed the highest and most stable color intensities on the test strips. The test strips did not produce enough coloration at pH values equal to or less than 5.0. At pH 10.0, the strips turned yellowish-brown, but the discoloration disappeared when the pH was increased above pH 10.0. This may be due to methomyl undergoing hydrolysis in basic conditions or structural changes in acidic conditions due to protonation (Tomašević et al., 2015). In a similar study, Bordbar and team (2020) reported that the optimum pH for the silver nanoparticle impregnated paper sensors is pH 9.00. A weak interaction at acidic and basic media can modify the nanoparticle surface charge, causing inconsistent color intensities in the paper sensors.

Dipping Time

Four (4) batches of test strips, each prepared in triplicate, were immersed in a 25.0 mg/L standard methomyl solution, with each batch subjected to varying dipping durations (5 s, 15 s, 30 s, and 60 s) (Figure 6C). After immersion, the strips were dried for two hours to ensure proper color fixation. The test strips immersed for 60 seconds showed more pronounced coloration, indicating that enough time was allowed for the methomyl molecules to interact with the reactive agents on the paper (Bordbar et al., 2020). Prolonged exposure ensured sufficient interaction between methomyl and the test strip reagents, resulting in more reliable color shifts. On the contrary, shorter immersion times (5-30 s) resulted in less intense coloration because of insufficient fixation of the methomyl on the strips. Furthermore, a Relative Standard Deviation (RSD) of 3.89% at 60 s was calculated, demonstrating minimal variation in the measurements, as RSD10% indicates good reproducibility (Bordbar, et al. 2020; Pang et al., 2022).

Drying Time

The test strips exposed to methomyl solution were hung and left to dry via air-drying, and the color intensities of the test strips were recorded every 10 min. ANOVA test revealed that there were no significant differences in the color intensities of the strips from 10 min to 120 min of drying time, with Fcalc= 0.17 < Fcrit= 2.22. For consistency, all test strips in the succeeding tests were dried for 80 min to ensure proper drying. Allowing adequate drying time ensures that the color response accurately represents the methomyl concentration. The RSD values of all recorded times are less than 10%.

Reproducibility of Assay Responses

The response of the test strips at varying methomyl concentrations are shown in Figure 6E. Visual inspection revealed that the color intensities within each set were closely comparable, as confirmed by the RSD values, which were below 10%, indicating minimal variations at different concentrations.

Stability Test

Significant color differences were observed after storing the used test strips for (a) 2 h, (b) 24 h, and (c) 48 h (Figure 6F). The ANOVA test revealed a significant difference in the mean color intensities of the varying storage durations with Fcalc= 7.3 > Fcrit= 5.14. Through visual inspection, the discoloration of the test strips is noticeable at 24 h, which changed further after 48 hr. This means that the used test strips should be read within 2 h as the color changes noticeably after24 h.

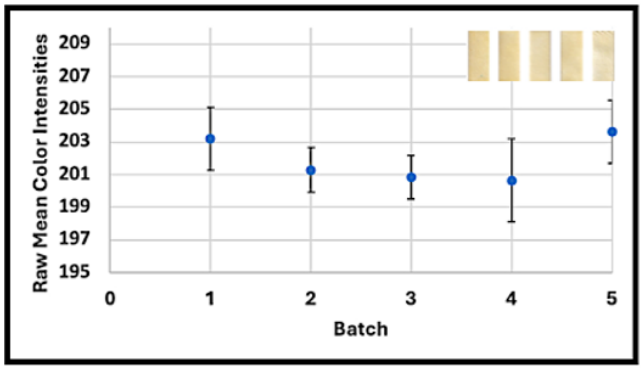

A. Initial color intensities of the fabricated test strips with Q-AgNP.

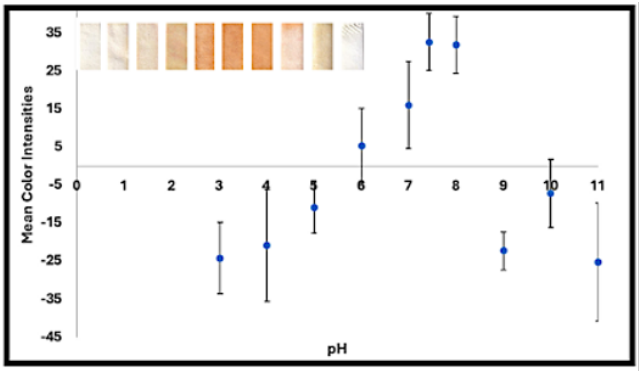

B. Effect of different pH levels: pH 3, 4, 5, 6, 7, 7.43 (initial), 8, 9, 10 and 11 to the color intensities of the strips.

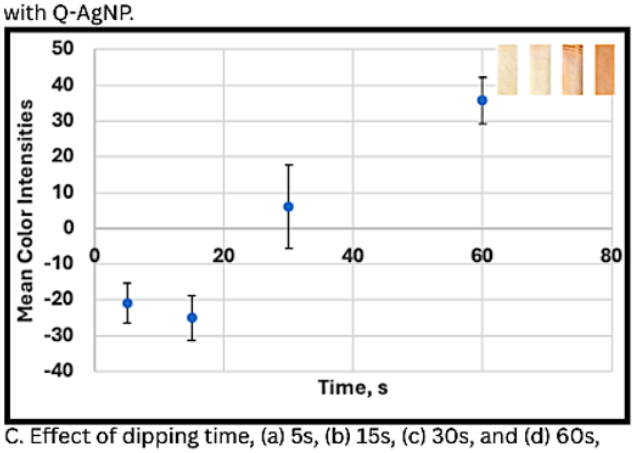

C. Effect of dipping time, (a) 5s, (b) 15s, (c) 30s, and (d) 60s, upon exposure to 25.0 ppm methomyl solution. .

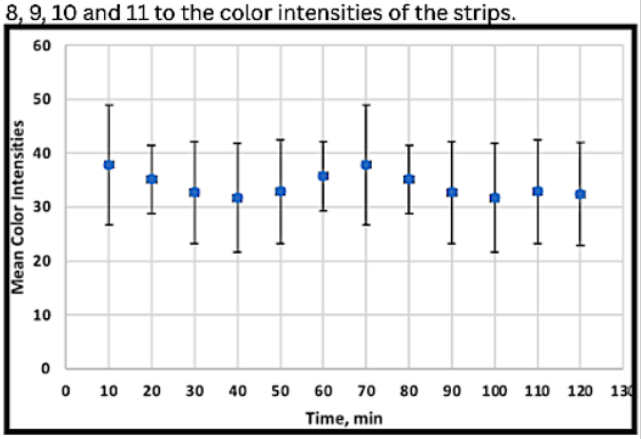

D. Effect of drying time, 10 to 120 min, after exposure to methomyl solution.

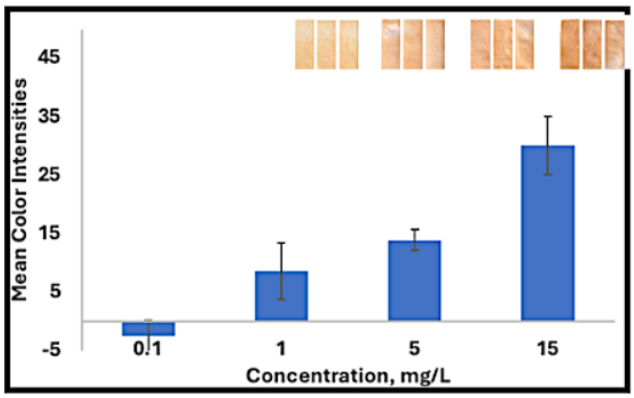

E. Effect of methomyl concentrations to the reproducibility of the color intensities.

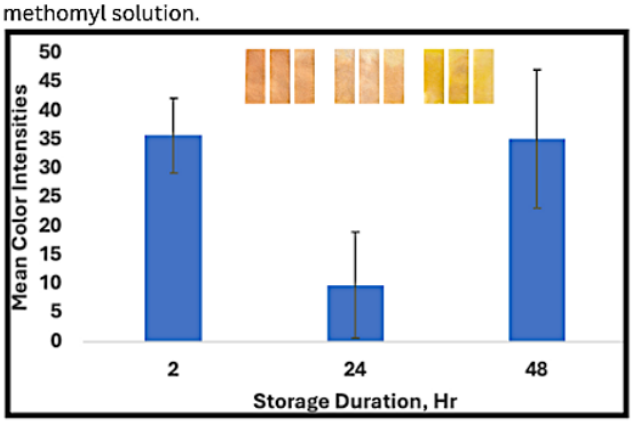

F. Effect of storage durations 2 hr, 24 hr, and 48 hr to the color intensities of the strips.

Figure 6: Optimization of the Paper-based Colorimetric Device.

Analytical Evaluation

Linear Range

The linear range for the standard methomyl solutions was revealed to be between 0.50 mg/L to 15.00 mg/L. The calibration curve equation based on the ΔRGB response has a correlation coefficient (R^2) of 0.9846 (Figure 7), proving the direct relationship of the color intensity of the strips to the methomyl concentration.

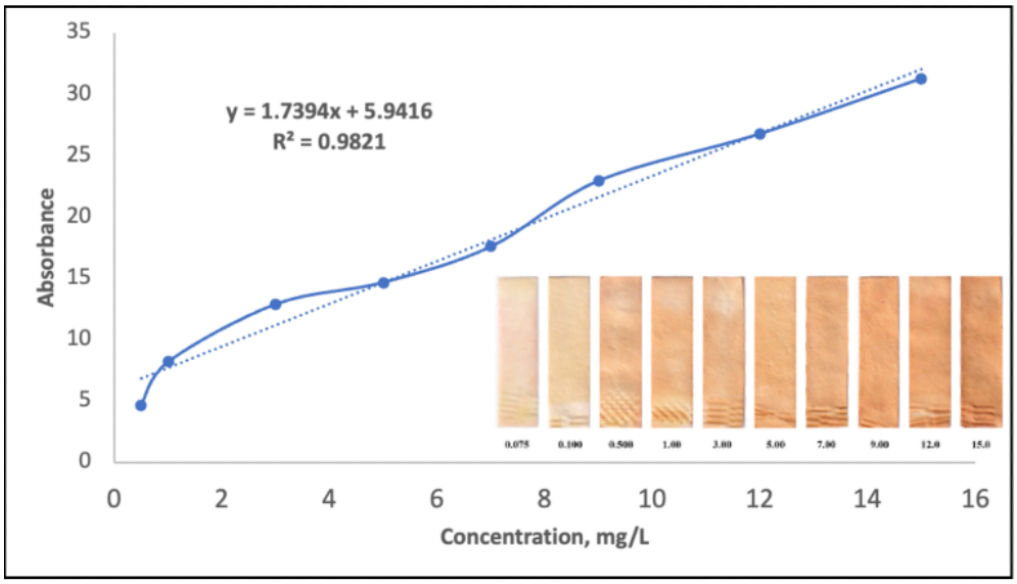

Figure 7: Linear range of the Standard Methomyl Concentrations as determined using the Paper-based Detector.

Limits of Detection (LOD) and Quantification (LOQ)

The Limit of Detection (LOD) and Limit of Quantification (LOQ) were calculated based on the calibration curve derived from lower methomyl concentrations ranging from0.50 mg/L to 5.00 mg/L, with a calibration curve of , y = 2.0722x + 5.0979. The LODof the fabricated device was calculated to be 2.621 mg/L, while the LOQ was 7.943 mg/L. In comparison, Bordbar and team (2020) used concentrations in the ng/mL range for the calibration curve and calculated lower LOD values for all the pesticides tested. In comparison, other paper-based devices showed lower LOD like the acetylcholine esterase-AgNP for the detection of profenofos which achieved an LOD of 0.04 mg/L when calculated from the calibration curve with standard concentrations ranging from 0.05 mg/L to 2.50 mg/L (Hermanto et al., 2023). Similar studies are shown in the table below.

Table 1: Related studies on paper-based devices for the detection of pesticide residues.

Authors and Research title	LOD and/or LOQ	Assay Method
This study	2.621 mg/L for the limit of detection and 7.943 mg/L for the limit of quantification.	Paper-based device impregnated with Quercetin-AgNP
Smartphone-coupled three-layered paper-based microfluidic chips demonstrating stereoscopic capillary-driven fluid transport towards colorimetric detection of pesticides (Wu et al., 2022)	34 nM (equivalent to 0.0055 mg/L) calculated from the linear range of 0.14-1.85 µmol/L (0.022 to 0.30 mg/L) for methomyl.	Smartphone-coupled three-layered paper-based microfluidic chip
A portable and automatic dual-readout detector integrated with 3D-printed microfluidic nanosensors for rapid carbamate pesticides detection (Zhao et al., 2021).	0.003102 mg/L for carbamate residues.	3D printed microfluidic chip with AuNP
A paper-based colorimetric sensor array for discrimination and simultaneous determination of organophosphate and carbamate pesticides in tap water, apple juice, and rice (Bordbar et al., 2020).	29.0, 22.0, 32.0, 17.0, 45.0, and 36.0 ng mL^{-1} (equivalent to 0.029 mg/L to 0.036 mg/L) for carbaryl, paraoxon, parathion, malathion, diazinon, and chlorpyrifos, respectively.	Paper-based devices of AgNP with L-Arginine, AuNP with L-Arginine, AgNP with quercetin, AuNP with quercetin, AgNP with PGA and AuNP with PGA
Bioactive Paper Sensor Based on the Acetylcholinesterase for the Rapid Detection of Organophosphate and Carbamate Pesticides (Badawy and Aswad, 2014).	The detection limit was 6.16×10^{-4} mM (0.100 mg/L) for methomyl by testing the inhibitory effect in the range of 6.16×10^{-8} and 0.620 mM (equivalent to $9.99x10^{-6}$ to 101 mg/L).	Biopolymer chitosan gel immobilized with glutaraldehyde as crosslinker, with AChE and 5,5′-dithiobis(2-nitrobenzoic) acid (DTNB) and acetylthiocholine iodide (ATChI)

The LOD of the fabricated paper-based device (2.621 mg/L) is higher than the detection limits reported by other studies, which typically reach the µg/L range. Nonetheless, this performance remains suitable for detecting methomyl at concentrations that may occur in highly contaminated agricultural runoff or freshly treated crops, which could be as high as 235.37 mg methomyl for every

1kg of plant material in the case of the spinach plant (Ramadan et al., 2021). However, the current sensitivity would limit the detection of minimal pesticide residues with concentrations lower than the LOD, which could happen if the crop was harvested several days after the treatment, as methomyl has a half-life of about 2-3 days (Ramadan et al., 2021; El-Hefny et al., 2019; EFSA, 2015).

Ultraviolet-Visible Spectrophotometry Analysis

A strong linear relationship was observed for Q-AgNP–methomyl standard solutions in the range of 0.075–15 mg/L, with the regression equation $y = 0.1787x + 0.0011$ and an R^2 of 0.9966, confirming the direct proportionality of the abs to the concentration. The calculated LOD LOQ using UV-Vis spectroscopy was 0.247 mg/L and 0.749 mg/L, respectively. In this study, however, UV-Vis spectroscopy was only used to verify the response of the paper-based device, rather than provide the full analytical validation. Because both techniques rely on a similar underlying mechanism, UV-Vis spectroscopy cannot be used as a reference method for analytical validation. Validation of such paper-based device requires more robust assessments of accuracy which can be provided by methods like chromatography.

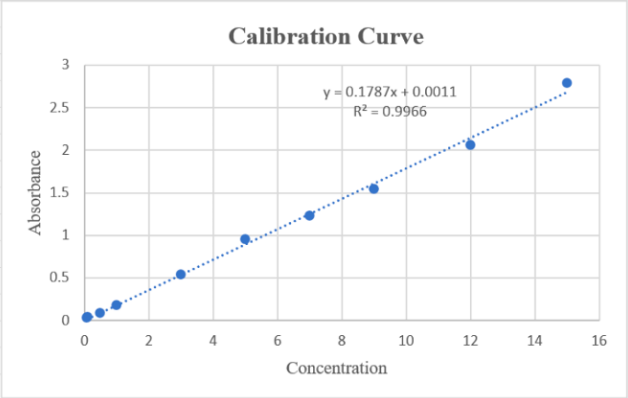

Figure 8: Calibration curve of Q-AgNP–methomyl standard solutions.

Spiked-Real Sample Analysis

Using the developed sensor, methomyl in the spiked eggplant samples was detected with mean recovery rates of 93.26% for 5 mg/L and 94.81% for 10 mg/L, respectively, while the recovery rates using the UV-Vis Spectrophotometer were 98.09% for 5 mg/L and 97.85% for 10 mg/L, respectively. These values fall within the acceptable analytical recovery range (80 – 110%), proving the reliability of the sensor in detecting methomyl at varying concentrations (Taverniers, et al., 2010). The Fcalc values for the comparison of the two methods in 5 mg/L and 10 mg/L concentrations exceeded the Fcrit values, which means that the two methods have significantly different variances, with UV-Vis spectroscopy demonstrating higher precision compared to the paper-based device as reflected by the lower variance and higher recovery rates (Figure 9). On the other hand, Welch's t-test confirms that their means are not statistically different, with two-tailed p-values of 0.391 (5 mg/L) and 0.447 (10 mg/L), which are both greater than the significance level of 0.05. Paper-based sensors are known to have low sensitivity, short linear range and higher susceptibility to error (Pang et al., 2022), primarily due to the inconsistent distribution of the reacting substance in the paper substrate. The statistical results suggest that although the response of the paper-based device shows more variation compared to the UV-Vis spectrophotometer, the mean responses of the two methods are comparable.

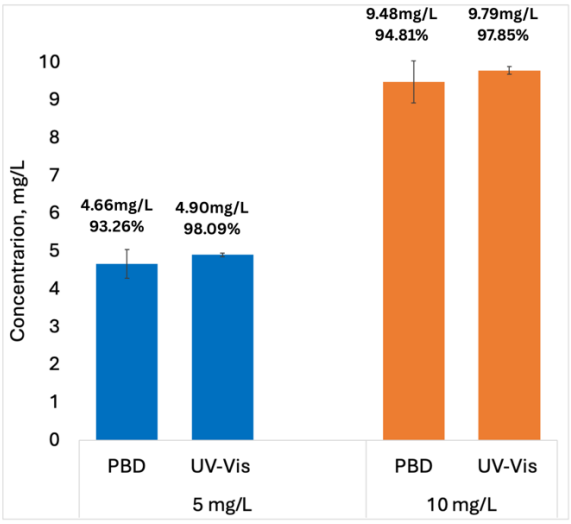

Figure 9: Comparison of the Recovery of the Paper Detector (PBD) and UV-Vis Spectroscopy at 5 mg/L and 10 mg/L.

CONCLUSION

In this study, a paper-based colorimetric sensor was developed to detect methomyl pesticide residues in eggplant samples using quercetin-modified silver nanoparticles (Q-AgNPs). This sensor relies on the principle of the optical properties of silver nanoparticle and the stabilizing function of quercetin and thus demonstrates a potential cost-effective alternative to the routine methods of pesticide detection. In addition, this paper-based device can potentially be used as a preliminary tool for detecting pesticide residues under field conditions, especially in areas where sophisticated laboratory equipment is scarce. Efforts were made to optimize the sensor for a more stable and reproducible performance. The best conditions were established as the pH being 7.43–8.00, dipping time of 60 s, and drying time of 80 min. In these conditions, the paper-based device had a linear detection range of 0.50–15.00 mg/L for methomyl with a R^2=0.9846, a LOD of 2.621 mg/L, and LOQ of 7.943 mg/L. The paper-based device recovered 93.26–94.81% of the methomyl concentration, which is statistically comparable to the results using the UV–Vis spectrophotometer (97.85–98.09%).

This comparability makes it a promising preliminary tool for rapid testing of pesticides on-site, however, it cannot replace established analytical techniques yet, especially if regulatory quantification is required. Overall, if the reagents are readily available, the test strips can be prepared in 125 min to ensure proper drying. The duration of sample preparation depends on the complexity of the sample, but the reaction with the strips can be done in 60 to 120 min, which mostly involves the drying of the strips. Its portability and ease of use can support safer agricultural practices and contribute to consumer health protection, especially in settings with limited resources, albeit needing improvements, which are mentioned in the recommendations below.

Since the paper-based device was only tested with methomyl, the response of the sensor with other carbamate pesticides should be determined. Large-scale sensor testing for various agricultural products other than eggplant must also be performed to determine its versatility and effectiveness in other food matrices. The duration of effectiveness of the reagents and the expiration of the fabricated test strips must also be determined to check if the strips can be prepared several days before the field analysis, which would lessen the time of preparation. LOD and LOQ of the sensor can also be determined by using blank replicate analysis, estimation using low concentrations of methomyl, or by using lower analyte concentrations in the formulation of the calibration curve. The

latter was used for this research due to the practicality of having a calibration curve based on the assumed linear range, but the calculated LOD was generally higher than those reported in the references. The use of lower standard concentrations could prevent this overestimation. Moreover, instead of using UV-Vis spectroscopy, chromatography is a better option in the verification of the sensor's response and analytical validation. However, such instrument was not available to the researchers during the conduct of this study. Other emerging techniques like smartphone digital imaging can be used to test the colorimetric response of the strips, to create a more portable and field-ready paper device. Lastly, the stability under various environmental factors such as temperature and humidity, should be further evaluated to further establish its usability in diverse environmental conditions.

ACKNOWLEDGMENT

The researchers would like to acknowledge the Chemistry Department of Tarlac State University for providing the opportunity to conduct this study.

CONFLICT OF INTEREST

The authors declare that there is no conflict of interest.

CONTRIBUTIONS OF INDIVIDUAL AUTHORS

I.M. Vasquez: Conceptualization; Experimentation; Procurement; Data Analysis; Writing-original draft and editing. **V. Escalona**: Conceptualization, Experimentation; Data Analysis; Writing-original draft and editing. **M.A. Liscano**: Experimentation; Data Analysis; Writing-original draft and editing. **A. Tabamo:** Project adviser; Conceptualization, Writing-review and editing.

REFERENCES

Badawy, M. E. I., & El-Aswad, A. F. (2014). Bioactive paper sensor based on the acetylcholinesterase for the rapid detection of organophosphate and carbamate pesticides. *International Journal of Analytical Chemistry, 2014*, 536823. https://doi.org/10.1155/2014/536823

Bhutto, A. A., Kalay, S., Sherazi, S. T. H., & Culha, M. (2018). Quantitative structure–activity relationship between antioxidant capacity of phenolic compounds and the plasmonic properties of silver nanoparticles. Talanta, 189, 174–181. https://doi.org/10.1016/j.talanta.2018.06.080

Bordbar, M. M., Nguyen, T. A., Arduini, F., & Bagheri, H. (2020). A paper-based colorimetric sensor array for discrimination and simultaneous determination of organophosphate and carbamate pesticides in tap water, apple juice, and rice. Microchimica Acta, 187(11), 594. https://doi.org/10.1007/s00604-020-04596-x

Chahardoli, A., Hajmomeni, P., Ghowsi, M., Qalekhani, F., Shokoohinia, Y., & Fattahi, A. (2021). Optimization of quercetin-assisted silver nanoparticles synthesis and evaluation of their hemocompatibility, antioxidant, anti-inflammatory, and antibacterial effects. Global Challenges, 5(12), 2100075. https://doi.org/10.1002/gch2.202100075

Chen, H., Shi, Q., Fu, H., et al. (2020). Rapid detection of five pesticide residues using complexes of gold nanoparticle and porphyrin combined with ultraviolet visible spectrum. Journal of the Science of Food and Agriculture, 100(12), 4464–4473. https://doi.org/10.1002/jsfa.10487

Dhavle, V., Kateshiya, M. R., Park, T.-J., & Kailasa, S. K. (2021). Functionalization of silver nanoparticles with carbohydrate derivative for colorimetric assay of thiram. Journal of Electronic Materials, 50(6), 3676–3685. https://doi.org/10.1007/s11664-021-08875-y

El-Hefny, D., Abdallah, I., Helmy, R., & Mahmoud, H. (2019). *Dissipation of methomyl residues in tomato fruits, soil and water using LC-MS/MS*. Journal of Plant Protection Research, 59(3), 355–361. https://doi.org/10.24425/jppr.2019.129742

European Food Safety Authority (EFSA). (2015). *Review of the existing maximum residue levels for methomyl according to Article 12 of Regulation (EC) No 396/2005*. EFSA Journal, 13(10), 4277. https://doi.org/10.2903/j.efsa.2015.4277

European Parliament and Council of the European Union. (2009). Regulation (EC) No 1107/2009. Official Journal of the European Union, 1–50.

Fertilizer and Pesticide Authority. (2024). Publication of updated list of registered pesticide products (pp. 1–398). https://fpa.da.gov.ph/wp-content/uploads/2024/05/Updated-List-of-Registered-pesticide-final-as-of-May-2-2024.pdf

Gupta, R. C. (2014). Carbamate pesticides. In Encyclopedia of toxicology (pp. 661–664). https://doi.org/10.1016/B978-0-12-386454-3.00106-8

Hermanto, D., Ismillayli, N., Hamdiani, S., Kamali, S. R., Wirawan, R., & Muliasari, H. (2023). Paper biosensors utilize silver nanoparticles for onsite pesticide residue detection. E3S Web of Conferences, 467, 01026. https://doi.org/10.1051/e3sconf/202346701026

Hoang, V.-T., Dinh, N. X., et al. (2021). Functionalized silver nanoparticles-based efficient colorimetric platform: Effects of surface capping agents on the sensing response of thiram pesticide in environmental water samples. Materials Research Bulletin, 139, 111278. https://doi.org/10.1016/j.materresbull.2021.111278

Jali, A. M. (2024). *Organophosphate and carbamate toxicity: Understanding, diagnosing and treating poisoning. Journal of Pioneering Medical Sciences, 13*(7), 89–103. https://doi.org/10.47310/jpms2024130714

Jana, J., Ganguly, M., & Pal, T. (2016). Enlightening surface plasmon resonance effect of metal nanoparticles for practical spectroscopic application. RSC Advances, 6(89), 86174–86211. https://doi.org/10.1039/c6ra14173k

Javed, R., Zia, M., Naz, S., Aisida, S. O., Ain, N. ul, & Ao, Q. (2020). Role of capping agents in the application of nanoparticles in biomedicine and environmental remediation: Recent trends and future prospects. Journal of Nanobiotechnology, 18(1), 1–15. https://doi.org/10.1186/s12951-020-00704-4

Khandel, P., Kumar Shahi, S., Kanwar, L., Kumar Yadaw, R., & Kumar Soni, D. (2018). Biochemical profiling of microbes inhibiting silver nanoparticles using symbiotic organisms. International Journal of Nano Dimension, 9(3), 273–285. https://doi.org/10.22034/IJND.2018.541895

Mahitha, B., Raju, B., Dillip, G. R., Reddy, C. M., Mallikarjuna, K., Manoj, L., & Sushma, N. (2011). *Biosynthesis, characterization and antimicrobial studies of AgNPs extract from Bacopa monniera whole plant. Digest Journal of Nanomaterials and Biostructures, 6*(1), 135-142

Mistry, H., Thakor, R., Patil, C., Trivedi, J., & Bariya, H. (2021). Biogenically proficient synthesis and characterization of silver nanoparticles employing marine procured fungi Aspergillus brunneoviolaceus along with their antibacterial and antioxidative potency. Biotechnology Letters, 43(1), 307–316. https://doi.org/10.1007/s10529-020-03008-7

Mohammadi, S., & Khayatian, G. (2017). Silver nanoparticles modified with thiomalic acid as a colorimetric probe for determination of cystamine. Microchimica Acta, 184(1), 253–259. https://doi.org/10.1007/s00604-016-1991-4

Moon, J. M., Chun, B. J., & Lee, B. K. (2012). Glasgow coma scale score in the prognosis of acute carbamate insecticide intoxication. Clinical Toxicology, 50(9), 832–837. https://doi.org/10.3109/15563650.2012.727093

Ngidlo, R. T. (2013). Impacts of pesticides and fertilizers on soil, tail water and groundwater in three vegetable producing areas in the Cordillera Region, northern Philippines. American Journal of Experimental Agriculture, 3(4), 780–793. https://doi.org/10.9734/ajea/2013/4696

Pandian, S. R. K., Kunjiappan, S., Ravishankar, V., & Sundarapandian, V. (2021). *Synthesis of quercetin-functionalized silver nanoparticles by rapid one-pot approach*. BioTechnologia, 102(1), 75–84. https://doi.org/10.5114/bta.2021.103764

Pang, R., Zhu, Q., Wei, J., Meng, X., & Wang, Z. (2022). *Enhancement of the detection performance of paper-based analytical devices by nanomaterials*. Molecules, 27(2), 508. https://doi.org/10.3390/molecules27020508

Rajhard, S., Hladnik, L., Vicente, F. A., Srčič, S., Grilc, M., & Likozar, B. (2021). Solubility of luteolin and other polyphenolic compounds in water, nonpolar, polar aprotic and protic solvents by applying FTIR/HPLC. Processes, 9(11), 1952. https://doi.org/10.3390/pr9111952

Ramadan, M. M., Fetoh, B. E.-S. A., & Ali, A. A. I. (2021). *Chlorfenapyr and methomyl deterioration on spinach plants and their residual effects in vitro on Egyptian cotton leafworm (Spodoptera littoralis)*. Journal of Nutrition and Food Processing, 4(7). https://doi.org/10.31579/2637-8914/068

Rohit, J. V., & Kailasa, S. K. (2014). Cyclen dithiocarbamate-functionalized silver nanoparticles as a probe for colorimetric sensing of thiram and paraquat pesticides via host–guest chemistry. Journal of Nanoparticle Research, 16(11), 2585. https://doi.org/10.1007/s11051-014-2585-x

Rowayshed, G., Sharaf, A., & Mostafa, M. (2013). Stability of carbamate pesticides residue in some vegetables throughout the household processing and cooking. Middle East Journal of Applied Sciences, 3(4), 205–215. https://www.curresweb.com/mejas/mejas/2013/205-215.pdf

Tasca, F., & Antiochia, R. (2020). Biocide activity of green quercetin-mediated synthesized silver nanoparticles. Nanomaterials, 10(5), 909. https://doi.org/10.3390/nano10050909

Taverniers, I., Van Bockstaele, E., & De Loose, M. (2010). Analytical method validation and quality assurance. In Pharmaceutical sciences encyclopedia (pp. 1–48). https://doi.org/10.1002/9780470571224.pse396

Tomašević, A., Gašić, S., Mijin, D., Petrović, S., Dugandžić, A., & Glavaški, O. (2015). *Removal of carbamate residues from water by different photochemical processes*. In D. Marčić, M. Glavendekić, & P. Nicot (Eds.), *Proceedings of the 7th Congress on Plant Protection* (pp. 371–376). Plant Protection Society of Serbia, IOBC-EPRS, IOBC-WPRS.

Upadhyay, P., Mishra, S. K., Purohit, S., Dubey, G. P., Chauhan, B. S., & Srikrishna, S. (2019). Antioxidant, antimicrobial and cytotoxic potential of silver nanoparticles synthesized using flavonoid rich alcoholic leaves extract of *Reinwardtia indica*. *Drug and Chemical Toxicology, 42*(1), 65-75. https://doi.org/10.1080/01480545.2018.1488859

U.S. Environmental Protection Agency, Office of Pesticide Programs. (2006, August 3). Reregistration eligibility decision for carbofuran (Case No. 0101; EPA-738-R-06-031). U.S. Environmental Protection Agency. https://archive.epa.gov/pesticides/reregistration/web/pdf/carbofuran_red.pdf

Wu, H., Chen, J., Yang, Y., Yu, W., Chen, Y., Lin, P., & Liang, K. (2022). Smartphone-coupled three-layered paper-based microfluidic chips demonstrating stereoscopic capillary-driven fluid transport towards colorimetric detection of pesticides. *Analytical and Bioanalytical Chemistry, 414*(5), 1759–1772. https://doi.org/10.1007/s00216-021-03839-x

Xia, J.-D., Wang, H., Hua, L.-W., Xu, M., Zheng, X., & Zhang, K. (2024). Comparative analysis of organophosphorus versus carbamate pesticide poisoning: A case study. *Arhiv za higijenu rada i toksikologiju*, *75*(1), 81–84. https://doi.org/10.2478/aiht-202x4-75-3781

Zhang, L., Zhang, Q., Liu, Q., Wu, X., Dong, Y., & Wang, G.-L. (2021). *Smart nanozyme of silver hexacyanoferrate with versatile bio-regulated activities for probing different targets*. Talanta, 228, 122268. https://doi.org/10.1016/j.talanta.2021.122268

Zhao, S., Huang, J., Lei, J., Huo, D., Huang, Q., Tan, J., Li, Y., Hou, C., & Tian, F. (2021). A portable and automatic dual-readout detector integrated with 3D-printed microfluidic nanosensors for rapid carbamate pesticides detection. *Sensors and Actuators B: Chemical, 346*, 130454. https://doi.org/10.1016/j.snb.2021.130454